Available online at www.sciencedirect.com
ScienceDirect
Coordination Chemistry Reviews 252 (2008) 244–258
COORDINATION CHEMISTRY REVIEWS
www.elsevier.com/locate/ccr

Review

Protein ligation of the photosynthetic oxygen-evolving center

Richard J. Debus *

Department of Biochemistry, University of California at Riverside, Riverside, CA 92521-0129, United States

Received 22 June 2007; accepted 26 September 2007
Available online 2 October 2007

Contents

Abstract

Photosynthetic water oxidation is catalyzed by a unique Mn_4Ca cluster in Photosystem II. The ligation environment of the Mn_4Ca cluster optimizes the cluster's reactivity at each step in the catalytic cycle and minimizes the release of toxic, partly oxidized intermediates. However, our understanding of the cluster's ligation environment remains incomplete. Although the recent X-ray crystallographic structural models have provided great insight and are consistent with most conclusions derived from earlier site-directed mutagenesis studies, the ligation environments of the Mn_4Ca cluster in the two available structural models differ in important respects. Furthermore, while these structural models and the earlier mutagenesis studies agree on the identity of most of the Mn_4Ca cluster's amino acid ligands, they disagree on the identity of others. This review describes mutant characterizations that have been undertaken to probe the ligation environment of the Mn_4Ca cluster, some of which have been inspired by the recent X-ray crystallographic structural models. Many of these characterizations have involved Fourier transform infrared (FTIR) difference spectroscopy because of the extreme sensitivity of this form of spectroscopy to the dynamic structural changes that occur during an enzyme's catalytic cycle.

Keywords: FTIR; Mn cluster; Oxygen evolution; Site-directed mutagenesis; Infrared spectroscopy; S-state cycle

Abbreviations: Chl, chlorophyll; DCMU, 3-(3,4-dichlorophenyl)-1,1-dimethylurea; EPR, electron paramagnetic resonance; ENDOR, electron nuclear double resonance; EXAFS, extended X-ray absorption fine structure; FTIR, Fourier transform infrared; P_{680}, chlorophyll species that serves as the light-induced electron donor in PSII; PSII, photosystem II; Q_A, primary plastoquinone electron acceptor; XANES, X-ray absorption near edge structure; Y_Z, tyrosine residue that mediates electron transfer between the Mn cluster and $P_{680}^{\bullet+}$; Y_D, second tyrosine residue in PSII that can rapidly reduce $P_{680}^{\bullet+}$.

* Tel.: +1 951 827 3483; fax: +1 951 827 4434.
E-mail address: richard.debus@ucr.edu.

0010-8545/$ – see front matter © 2007 Elsevier B.V. All rights reserved.
doi:10.1016/j.ccr.2007.09.022

1. Introduction

Attempts to identify the ligands of the Mn and Ca ions in photosystem II began shortly after the discovery that the D1/D2 heterodimer contains both P_{680} and Pheo and supports light-induced charge-separation [1,2]. All conserved Asp, Glu, and His residues in the lumenal domains of the D1 and D2 subunits were targeted subsequently by site-directed mutagenesis, mostly in *Synechocystis* sp. PCC 6803, a mesophilic cyanobacterium, but also in *Chlamydomonas reinhardtii*, a green alga. Other conserved residues and regions were also targeted. Mutations are now also being constructed in *Thermosynechococcus elongatus*, the thermophilic cyanobacterium that was used in the recent X-ray crystallographic studies [3,4]. Because of initial difficulties with isolating and purifying PSII particles having functionally intact oxygen evolving complexes from many of the mutants, most mutants were originally characterized by non-invasive methods *in vivo*, primarily by measuring changes in the yield of chlorophyll *a* fluorescence produced by flash or continuous illumination given in the presence or absence of DCMU. The subsequent development of improved methods for purifying PSII particles with conventional chromatography [5] and with metal ion affinity chromatography [6–8] has facilitated the characterization of mutants with a variety of spectroscopic methods such as time-resolved optical absorption spectroscopy, various forms of pulsed EPR spectroscopy, and FTIR difference spectroscopy. Characterizations are now also employing XANES, EXAFS, and time-resolved mass spectrometry. On the basis of the mutant characterizations that had been conducted by late 2003, the residues D1-Asp170, D1-His332, D1-Glu333, D1-His337, D1-Asp342, and the carboxyl-terminus of the D1 polypeptide at D1-Ala344 had been identified as possible ligands of Mn, the residues D1-Asp59, D1-Asp61, and D1-Asp342 had been identified as possible ligands of Ca, D1-Glu189 had been identified as a likely participant in a network of hydrogen bonds that facilitates electron transfer from the Mn_4Ca cluster to $Y_Z^{\bullet}$ during the higher S state transitions, and D1-His190 had been identified as the proton acceptor for Y_Z (for review, see Refs. [9–11]). The recent ~3.5 Å [3] and ~3.0 Å [4] X-ray crystallographic structural models support many of these proposals (*e.g.*, see Fig. 1), but conflict with others, most notably the ligation of Ca and the role of D1-Glu189. The main points of agreement and disagreement between the mutagenesis studies and recent X-ray crystallographic structural models are among the points that are discussed in this review.

Before undertaking detailed descriptions of mutants and their characterizations, it is worth mentioning that the ligation environment of the Mn_4Ca cluster in the recent ~3.5 Å and ~3.0 Å structural models differ in a number of respects. For example, most of the carboxylate metal ligands are unidentate in the ~3.5 Å structural model [3], whereas most of the carboxylate metal ligands bridge two metal ions in the ~3.0 Å structural model [4] (see Fig. 1). These differences are probably caused by differences in data quality, extent of radiation damage, and approach to interpreting the electron density. Regarding radiation damage, a recent polarized EXAFS study of PSII single crystals (conducted with X-ray doses below the thresholds that cause radiation-induced reduction of the cluster's Mn(III) and Mn(IV) ions) has provided compelling evidence that the structure of the Mn_4Ca cluster in native PSII preparations differs significantly from those depicted in either X-ray crystallographic structural model [12]. This study confirms earlier XANES and EXAFS studies of PSII single crystals [13] and PSII membrane multilayers [14] that provided compelling evidence that the X-ray doses that were used to irradiate the PSII crystals in the crystallographic studies would have rapidly reduced the Mn_4Ca cluster's Mn(III) and Mn(IV) ions to their fully reduced Mn(II) states and significantly perturbed the structure of the Mn_4Ca cluster, disrupting μ-oxo bridges and altering Mn-ligand interactions [13,14]. Consequently, the ligation environment of the native Mn_4Ca cluster may differ in important respects from the ligation environments that are depicted in the ~3.5 Å and ~3.0 Å structural models.

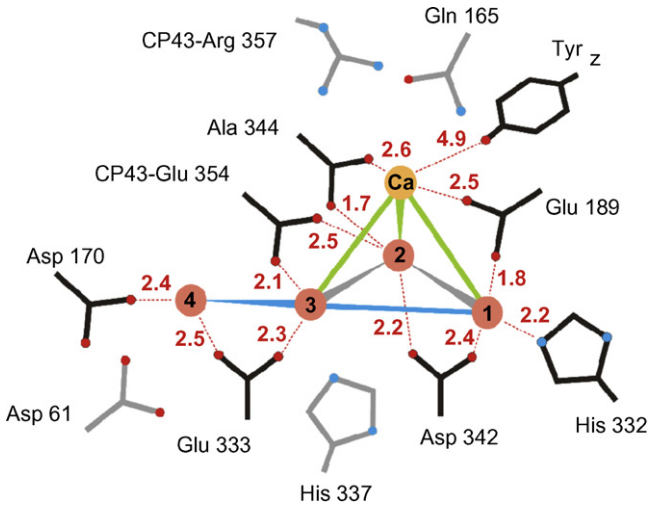

Fig. 1. Schematic view of the Mn_4Ca cluster and its protein environment as depicted in the 3.0 Å X-ray crystallographic structural model. Distances between Mn (red) and Ca (orange) ions in this model are indicated by the connecting lines (grey, 2.7 Å; blue, 3.3 Å; green, 3.4 Å). Amino acid residues in the first coordination sphere are black; those in the second sphere are grey. Distances are given in Ångstroms (reprinted with permission from Ref. [4], copyright 2005 by Macmillan Publishers Ltd., Nature Publishing Group).

Despite these ambiguities, the new structural models mark a new era in which mechanistic hypotheses can be developed and tested in the light of insights derived from structural information. In addition, the new models are serving as valuable guides for experiments designed to identify the specific Mn ion(s) that undergo oxidation during each step in the S state cycle, to identify the amino acid residues that facilitate the deprotonation and oxidation of the Mn_4Ca cluster during the individual steps of the S state cycle, and to identify the amino acid residues that participate in proton transfer pathways leading from the Mn_4Ca cluster to the thylakoid lumen. Many of these experiments involve mutant characterization with Fourier Transform Infrared (FTIR) difference spectroscopy. FTIR difference spectroscopy is an extremely sensitive tool for characterizing dynamic structural changes that occur during an enzyme's catalytic cycle, such as changes in molecular interactions, protonation states, bonding (including changes in

metal coordination and hydrogen bonding), bond strengths, and protein backbone conformations [15–18]. In PSII, numerous vibrational modes change as the Mn_4Ca cluster is oxidized through the S state cycle (for reviews, see refs [19–22]). Many of these vibrational modes are expected to correspond to amino acid residues that either ligate the Mn_4Ca cluster, are coupled to the Mn_4Ca cluster through hydrogen bonds, interact electrostatically with the Mn_4Ca cluster, or have side chains whose protonation states change as the Mn_4Ca cluster is oxidized. Identifying the vibrational modes that change during the S state cycle in PSII will provide information about S state-dependent protein structural changes. Such information will complement X-ray crystallography and provide insight into how the Mn_4Ca cluster's protein environment regulates the cluster's reactivity, matching its potential to that of Y_Z in each S state and minimizing the release of toxic, highly reactive, partly oxidized intermediates.

2. Protein ligation of manganese

2.1. The C-terminus of the D1 polypeptide at alanine 344

The free carboxylate (α-COO^-) of Ala344 at the C-terminus of the D1 polypeptide was first proposed to ligate the Mn cluster in 1992 on the basis of a study of cyanobacterial and algal mutants having truncated or unprocessed C-terminii [23]. To test this proposal, the mid-frequency S_2-*minus*-S_1 FTIR difference spectra of unlabeled and L-[1-^{13}C]alanine-labeled wild-type *Synechocystis* PSII particles were compared to determine if the vibrational modes that are altered during the $S_1 \rightarrow S_2$ transition include those of the α-COO^- group of D1-Ala344.[1] Two independent FTIR studies showed that the incorporation of L-[1-^{13}C]alanine altered the wild-type S_2-*minus*-S_1 mid-frequency FTIR difference spectrum, but only in the symmetric carboxylate stretching [$\nu_{sym}(COO^-)$] region [24,25] (see Fig. 2, top traces). The ^{12}C-*minus*-^{13}C double difference spectrum of this region (Fig. 3) showed that the alterations represent the ^{13}C-induced shift of a *single* vibrational mode. In the S_1 state, this mode appears at ∼1354 cm^{-1} and is shifted by ^{13}C to either ∼1338 cm^{-1} or ∼1320 cm^{-1}. In the S_2 state, this mode appears at either ∼1338 cm^{-1} or ∼1320 cm^{-1} and is shifted by ^{13}C to ∼1307 cm^{-1}. These data show that the $\nu_{sym}(COO^-)$ mode of D1-Ala344 in unlabeled, wild-type PSII particles shifts to lower frequency during the $S_1 \rightarrow S_2$ transition. This mode could be assigned unambiguously to the α-COO^- group of Ala344 because the mode was *not* shifted by the incorporation of L-[1-^{13}C]alanine into either D1-Ala344Gly or D1-Ala344Ser PSII particles [24,25] (the C-terminal α-COO^- group of the D1 polypeptide cannot be labeled in either mutant because it is no longer provided by alanine).

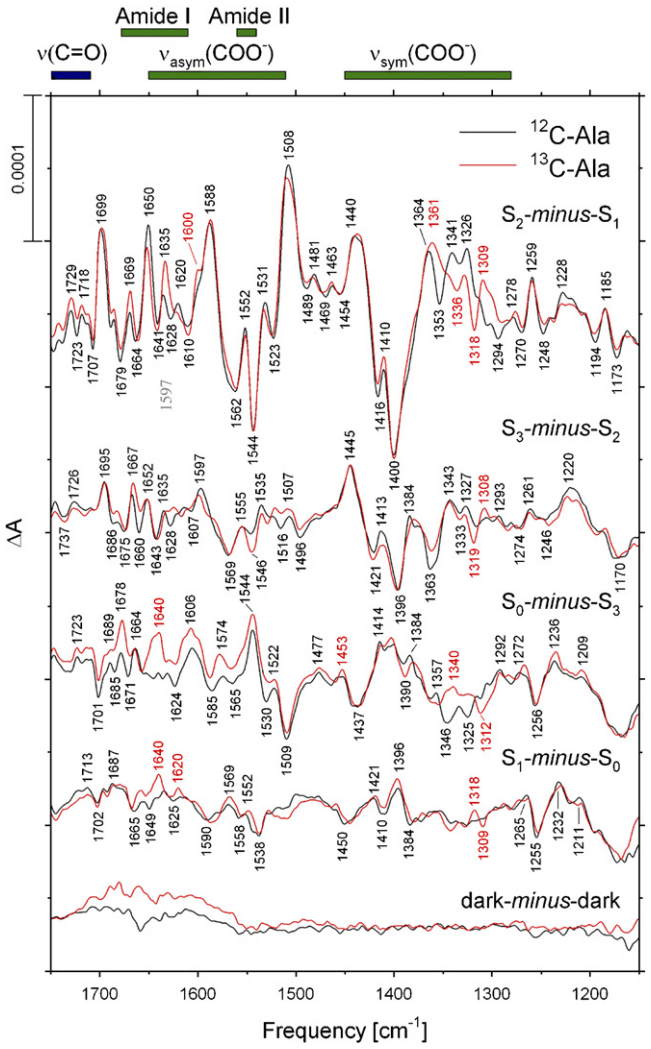

Fig. 2. Comparison of the S_{n+1}-*minus*-S_n FTIR difference spectra of wild-type PSII particles purified from *Synechocystis* sp. PCC 6803 cells that had been propagated in media containing unlabeled L-alanine (12C, black) or L-[1-^{13}C]alanine (red). The data were collected as described in Ref. [46] and show the averages of six unlabeled and six L-[1-^{13}C]alanine-labeled samples. The sample temperature was 273 K.

The $\nu_{sym}(COO^-)$ mode of free ionic amino acid residues appear near 1412 cm^{-1} [26]. Because the α-COO^- group of D1-Ala344 appears at ∼1354 cm^{-1} in the S_1 state and at ∼1338 cm^{-1} or ∼1320 cm^{-1} in the S_2 state, this mode is downshifted by ∼58 cm^{-1} in the S_1 state and by ∼74 cm^{-1} or ∼92 cm^{-1} in the S_2 state compared to the position of this mode in free ionic alanine. In metal–carboxylate complexes, the frequencies of the symmetric and asymmetric carboxylate stretching modes and the difference in frequency between them vary significantly with the metal ion and the type of carboxylate coordination [27–31]. For unidentate ligation, the position of the $\nu_{sym}(COO^-)$ mode is usually shifted 30–100 cm^{-1} to lower frequencies compared its value in free ionic carboxylates. Because the $\nu_{sym}(COO^-)$ mode of the α-COO^- group of D1-Ala344 is downshifted by ∼58 cm^{-1} in the S_1 state and by ∼74 cm^{-1} or ∼92 cm^{-1} in the S_2 state, it was concluded that the α-COO^-

[1] It was expected that, if the α-COO^- group of D1-Ala344 ligates the Mn_4Ca cluster, one or both of this group's carboxylate stretching modes might shift in frequency during the $S_1 \rightarrow S_2$ transition, causing them to appear in the S_2-*minus*-S_1 FTIR difference spectrum. The specific incorporation of L-[1-^{13}C]alanine would be expected to change the frequencies of *only* these modes, permitting their detection.

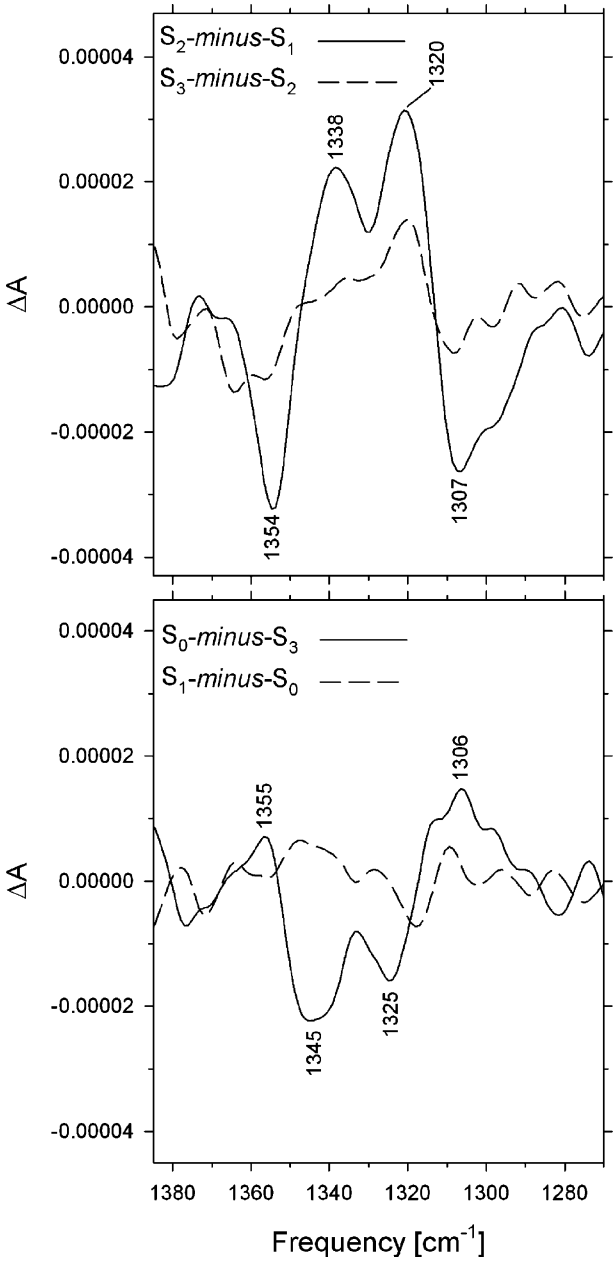

Fig. 3. Double difference spectra, ^{12}C-*minus*-^{13}C, obtained by subtracting the S_{n+1}-*minus*-S_n FTIR difference spectrum of L-[1-^{13}C]alanine-labeled PSII particles from that of unlabeled PSII particles (data from Fig. 1). Only the regions between 1385 cm^{-1} and 1270 cm^{-1} are shown. Note that the shift of the $\nu_{sym}(COO^-)$ mode of D1-Ala344 (from 1354 cm^{-1} to either 1338 cm^{-1} or 1320 cm^{-1}) that occurs during the $S_1 \rightarrow S_2$ transition is largely reversed during the $S_3 \rightarrow S_0$ transition.

group of D1-Ala344 is a unidentate ligand of a metal ion in both the S_1 and S_2 states [24,25]. Indeed, no mechanism other than unidentate ligation of a metal ion can account for the magnitude of the observed downshifts[2] except for asymmetric bidentate chelation of a metal ion, where the two metal–oxygen distances

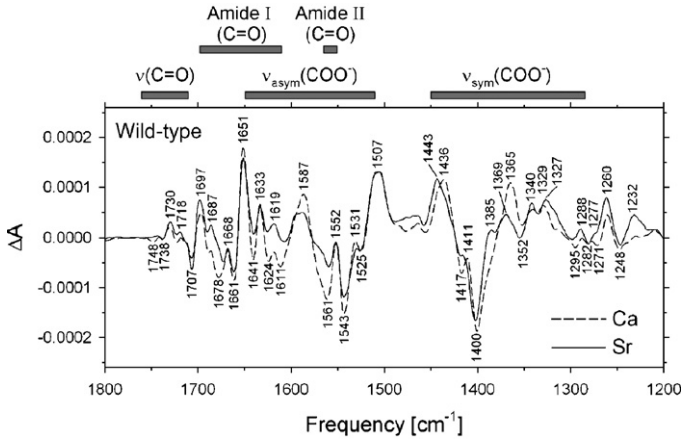

Fig. 4. Comparison of the mid-frequency S_2-*minus*-S_1 FTIR difference spectra of PSII particles purified from *Synechocystis* sp. PCC 6803 cells that had been propagated in media containing Ca (dashed) or Sr (solid). Each trace represents the average of six samples. The sample temperature was 250 K (modified from Ref. [32], reprinted with permission, copyright 2005 by the American Chemical Society).

are substantially different, a situation that does not seem to be very common [31].

As stated in the previous paragraph, the observed frequencies of the $\nu_{sym}(COO^-)$ mode of the α-COO$^-$ group of D1-Ala344 in the S_1 and S_2 states imply that the α-COO$^-$ group Ala344 is a unidentate ligand of a metal ion in both states. In wild-type PSII particles, this mode downshifts by ∼16 cm^{-1} or ∼34 cm^{-1} during the $S_1 \rightarrow S_2$ transition [24,25][3] and is restored during the $S_3 \rightarrow S_0$ transition (see Figs. 2 and 3 and Ref. [25]). These observations imply that the ligating C–O bond weakens during the $S_1 \rightarrow S_2$ transition and is restored during the $S_3 \rightarrow S_0$ transition. This weakening of the ligating C–O bond was attributed to the increased charge that develops on the Mn_4Ca cluster during the $S_1 \rightarrow S_2$ transition, although it has also been attributed to the elimination of Jahn–Teller distortion when the ligated Mn(III) ion undergoes oxidation to Mn(IV) (see Section 4). Consequently, it has been concluded that the α-COO$^-$ group of Ala344 ligates a Mn ion whose charge or formal oxidation state increases during the $S_1 \rightarrow S_2$ transition [24,25].

The original [1-^{13}C]alanine-labeling study [24] was conducted before the ∼3.5 Å X-ray crystallographic structural model was announced. In this structural model, the α-COO$^-$ group of Ala344 ligates no metal ion, but is located near the Mn_4Ca cluster's Ca ion [3]. To reassess whether the α-COO$^-$ group of Ala344 ligates Mn or Ca, wild-type cells of *Synechocystis* sp. PCC 6803 were propagated in the presence of Sr and either [1-^{13}C]alanine or unlabeled alanine [32]. This study showed that the substitution of Sr for Ca significantly alters several symmetric and asymmetric carboxylate stretching modes

[2] The possibility that the observed downshifts could be caused by the α-COO$^-$ group being protonated or involved in a strong hydrogen bond could be discounted [24].

[3] It is not yet possible to distinguish whether specific L-[1-^{13}C]alanine-labeling downshifts the symmetric carboxylate stretching mode of the α-COO$^-$ group of D1-Ala344 by ∼16 cm^{-1} or ∼34 cm^{-1} in response to the $S_1 \rightarrow S_2$ transition. Nevertheless, preliminary data obtained with CP43-Glu354Gln PSII particles suggests that this mode shifts by ∼16 cm^{-1} in response to the $S_1 \rightarrow S_2$ transition and that the incorporation of ^{13}C shifts this mode by ∼34 cm^{-1} (M.A. Strickler, R.J. Debus, unpublished).

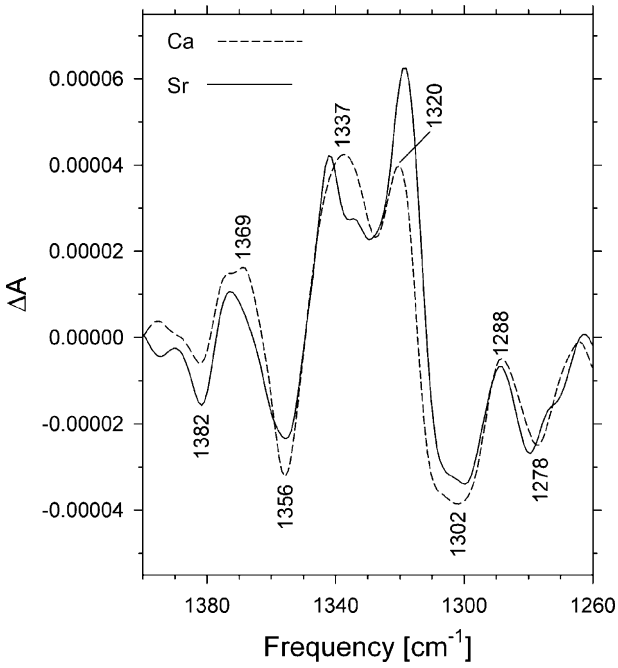

Fig. 5. Double difference spectra, ^{12}C-*minus*-^{13}C, of PSII particles containing Ca (dashed) or Sr (solid) obtained by subtracting the S_2-*minus*-S_1 FTIR difference spectra of L-[1-^{13}C]alanine-labeled PSII particles from the S_2-*minus*-S_1 FTIR difference spectra of unlabeled PSII particles. Only the regions between 1400 cm^{-1} and 1260 cm^{-1} are shown (modified from Ref. [32], reprinted with permission, copyright 2005 by the American Chemical Society).

(see Fig. 4), including some that may correspond to one or more metal ligands, but importantly does *not* alter the $\nu_{sym}(COO^-)$ mode of the α-COO^- group of D1-Ala344 [32] (see Fig. 5). Because it seems highly improbable that the structural perturbations of the oxygen evolving complex that are induced by substituting Sr for Ca (including the perturbation of multiple carboxylate groups, now demonstrated by several laboratories [32–34]) would not also alter the $\nu_{sym}(COO^-)$ mode of a carboxylate residue that is directly coordinated to the Ca ion, it was concluded that D1-Ala344 ligates Mn rather than Ca [32].[4] This conclusion is consistent with the 3.0 Å crystallographic structural model. In this model, the α-COO^- group of D1-Ala344 interacts strongly with a Mn ion (one oxygen is located 1.7 Å from Mn_2) and only weakly with the Ca ion (the other oxygen is located 2.6 Å from Ca) [4] (see Fig. 1).

Several D1-Ala344 mutants have been reported, including the D1-Ala344stop truncation mutant [23,37–39], D1-Ala344Gly [24,25,40,41], D1-Ala344Ser [24], D1-Ala344Asp [41], and others [41]. These studies have shown that the D1-Ala344 stop mutation, which truncates the D1 polypeptide by a single residue, prevents the stable assembly of the Mn_4Ca cluster [23,37,38] and slightly lowers the affinity of the high-affinity binding site for the first Mn(II) ion that is photooxidized during the light-driven assembly of the Mn_4Ca cluster [39]. This high-affinity site contains D1-Asp170 (see Section 2.2). This slightly lower affinity of the high-affinity site for Mn(II) ions appears to be a general feature of mutations constructed in the C-terminal domain of the D1 polypeptide [39] (see Sections 2.4–2.7). This lowered affinity implies that the C-terminal region of the D1 polypeptide is located near D1-Asp170 in the apo-protein and suggests that this region either increases the local concentration of Mn(II) ions near the D1-Asp170 high-affinity site or stabilizes a conformation that optimizes the affinity of this site for Mn(II) ions [39].

Replacing D1-Ala344 with other residues (Gly, Ser, Val, Asp, Asn) introduces minor spectral perturbations into the mid-frequency S_2-*minus*-S_1 FTIR spectrum [24,40]. Furthermore, the mutations D1-Ala344stop [25] and D1-Ala344Gly [40] perturb the low-frequency S_2-*minus*-S_1 FTIR spectrum between 640 cm^{-1} and 570 cm^{-1}. However, the significance of the mid- and low-frequency spectral perturbations is unclear because minor alterations to mid-frequency S_{n+1}-*minus*-S_n FTIR difference spectra appear to be produced by many or all mutations, even when constructed at a site far from the Mn_4Ca cluster [42]. Low-frequency spectral alterations similar to those reported in D1-Ala344stop and D1-Asp344Gly PSII particles have also been reported in D1-Asp170His [43] and D1-Glu189Gln [44] PSII particles (see Sections 2.2 and 2.4) and in samples having Sr substituted for Ca [45]. These spectral alterations have been attributed to indirect structural perturbations of a single Mn–O–Mn cluster mode [42,43,45,46].

2.2. Aspartate 170 of the D1 polypeptide

Aspartate-170 of the D1 polypeptide provides part of the high-affinity binding site for the first Mn(II) ion that is photooxidized during the light-driven assembly of the Mn_4Ca cluster [47–49]. This residue was predicted to ligate Mn on the basis of numerous mutagenesis studies (reviewed in Refs. [9–11]) and is a unidentate ligand of a single Mn ion in both recent X-ray crystallographic structural models [3,4] (see Fig. 1). However, no spectroscopic evidence that D1-Asp170 ligates the *assembled* Mn_4Ca cluster has yet been found (*e.g.*, see [50]).[5] Numerous spectroscopic studies have focused on the mutant D1-Asp170His. This mutant is weakly photoautotrophic and assembles Mn_4Ca clusters in ∼50% of its PSII reaction centers. These assembled Mn_4Ca clusters function normally [47,52,53] and exhibit normal S_1 and S_2 state multiline EPR signals [50]. In addition, two FTIR studies have shown that the S_2-*minus*-S_1 FTIR difference spectrum of D1-Asp170His PSII particles is essentially unchanged from that of wild-type PSII particles [43,46]. However, a low frequency vibrational mode that appears at ∼606 cm^{-1} in the S_2 state in wild-type PSII particles shifts to ∼612 cm^{-1} in D1-Asp170His PSII particles [43]. Similar spectral changes have been observed in D1-Ala344stop and D1-Ala344Gly PSII particles [25,40] (see Section 2.1), D1-

[4] It should be noted that some authors continue to assert that the α-COO^- group of D1-Ala344 ligates Ca rather than Mn [35,36].

[5] To explain the ability of D1-Asp170Val cells to grow photoautotrophically and the ability of D1-Asp170Leu and D1-Asp170Ile cells to evolve O_2 [51] despite the apparent role of D1-Asp170 as a ligand to Mn, it was proposed that the relative bulk and hydrophobicity of Val, Leu, and Ile cause structural perturbations that permit the missing D1-Asp170 carboxylate group to be replaced by another residue, a peptide carbonyl, or a water molecule [51].

Glu189Gln PSII particles [44] (see Section 2.3), and in PSII preparations having Sr substituted for Ca [45]. These spectral changes have been attributed to indirect structural perturbations of a single Mn–O–Mn cluster mode [42,43,45,46].

The announcement of the ~3.5 Å X-ray crystallographic structural model in 2003 inspired further FTIR studies of the D1-Asp170His mutant. The proximity of D1-Asp170 to Y_Z, to the Ca ion, and to a putative proton transfer pathway leading to the thylakoid lumen in this structural model [3], led to mechanistic proposals postulating that the Mn ion that is ligated by D1-Asp170 undergoes oxidation during one or more of the $S_0 \rightarrow S_1$, $S_1 \rightarrow S_2$, and $S_2 \rightarrow S_3$ transitions [36,54–58]. To test these proposals, the mid-frequency (1800–1000 cm^{-1}) S_1-*minus*-S_0, S_2-*minus*-S_1, S_3-*minus*-S_2, and S_0-*minus*-S_3 FTIR difference spectra of D1-Asp170His PSII particles were compared with those of wild-type PSII particles. The rationale was that, if D1-Asp170 ligates a Mn ion whose charge or oxidation state increases during a particular $S_n \rightarrow S_{n+1}$ transition, then the ligating Mn–O bond(s) would weaken during that transition (like that of D1-Ala344), thereby decreasing the frequency of the D1-Asp170 symmetric carboxylate stretching mode and possibly shifting the frequency of the D1-Asp170 asymmetric carboxylate stretching mode. The shifted mode(s) should appear in the corresponding S_{n+1}-*minus*-S_n FTIR difference spectrum of wild-type PSII particles but not in the spectrum of D1-D170H PSII particles, thereby permitting its(their) identification. Surprisingly, the mutation did not significantly alter *any* of the difference spectra (Fig. 6). Importantly, there was no indication that the D1-Asp170His mutation eliminates any carboxylate modes or creates any new histidyl modes.

The simplest explanation of the FTIR data is that D1-Asp170 ligates a Mn ion that does not increase its charge or oxidation state during any of the $S_0 \rightarrow S_1$, $S_1 \rightarrow S_2$, or $S_2 \rightarrow S_3$ transitions. If correct, this explanation would have profound implications for the mechanism of water oxidation because it would imply either that the oxidation of the Mn ion that is ligated by D1-Asp170 occurs only during the transitory $S_3 \rightarrow S_4$ transition, or that the oxidation increments and O_2 formation chemistry that occur during the catalytic cycle involve only the remaining Mn_3Ca portion of the Mn_4Ca cluster. However, three other explanations of the FTIR data have been considered. One is that D1-Asp170 does not ligate the *assembled* Mn_4Ca cluster. In view of the earlier mutagenesis studies and the recent X-ray crystallographic models, this possibility seems unlikely. Furthermore, because D1-Asp170 forms part of the binding site of the first Mn(II) ion that is incorporated into the Mn_4Ca cluster [47–49], this explanation would require that a structural rearrangement separate D1-Asp170 from the photooxidized Mn(III) ion as the Mn_4Ca cluster is formed. There is no precedent for such a rearrangement in any metalloenzyme except ferritin [59,60], where the change in Fe ligation is associated with ferritin's function as an iron storage protein. In PSII, there is no apparent need for separating D1-Asp170 from Mn during the assembly of the Mn_4Ca cluster.

A second alternate explanation for the FTIR data is that, although D1-Asp170 ligates the Mn_4Ca cluster, D1-His170 does not. In this scenario, the Mn-ligating carboxylate oxygen of D1-Asp170 is replaced in the D1-Asp170His mutant by an oxygen atom from another residue, a water molecule, by another group. However, it is difficult to understand why the high-affinity Mn(II) binding site would be retained in D1-Asp170His PSII particles [47,49], but not in D1-Asp170Asn, D1-Asp170Ala, or D1-Asp170Ser PSII particles [47,48], where the ligating D1-Asp170 carboxylate oxygen could *also* be replaced by an oxygen atom from another residue, a water molecule, or by another group. One would need to postulate that D1-His170 separates from the bound Mn(II) ion after it become oxidized because Mn(III) and Mn(IV) ions prefer harder Lewis bases as ligands. However, this reasoning does not seem compelling because (1) dimanganese catalase enzymes contain two Mn(III) ions at their active sites and each Mn(III) ion is directly coordinated to a histidyl nitrogen [61,62] and (2) D1-His332 is believed to ligate a Mn(III) or Mn(IV) ion (see Fig. 1 and Section 2.4). Another difficulty with this explanation is that it seems unlikely that replacing D1-Asp170 with another molecule would have no appreciable affect on the wealth of spectral features that are observed in all of the S_{n+1}-*minus*-S_n FTIR difference spectra (but see next paragraph).

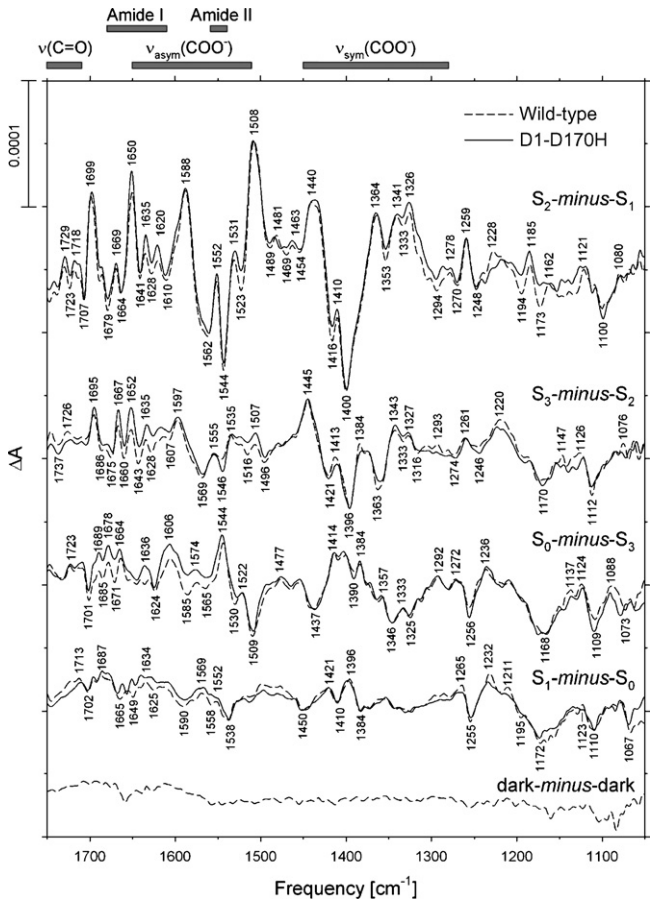

Fig. 6. Comparison of the S_{n+1}-*minus*-S_n FTIR difference spectra of wild-type (dashed) and D1-Asp170His (solid) PSII particles purified from *Synechocystis* sp. PCC 6803. The spectra have been normalized to maximize overlap. A dark-*minus*-dark control trace of the wild-type PSII particles is included to show the noise level (lower trace). The data (plotted from 1750 cm^{-1} to 1050 cm^{-1}) show the averages of 6 wild-type and 18 D1-Asp170His samples. The sample temperature was 273 K (modified from Ref. [46], reprinted with permission, copyright 2005 by the American Chemical Society).

A third alternative explanation for the FTIR data, favored by some authors [36,55,58], is that D1-Asp170 ligates a Mn ion that undergoes oxidation during one or both of the $S_0 \rightarrow S_1$ and or $S_2 \rightarrow S_3$ transitions, but the increased charge that develops on the Mn ion that undergoes oxidation is offset by the deprotonation of a water-derived ligand or water molecule. A difficulty with this explanation is that the Mn_4Ca cluster undergoes significant structural changes during the $S_2 \rightarrow S_3$ transition [63,64]. Some authors have proposed that these structural changes involve the creation of an additional di-μ-oxo bridge between Mn ions [64]. Smaller structural changes also accompany the $S_0 \rightarrow S_1$ transition [64,65]. If D1-Asp170 ligates the Mn ion that undergoes oxidation during the $S_0 \rightarrow S_1$ or $S_2 \rightarrow S_3$ transitions, it seems unlikely that the structural changes that accompany these transitions would not also alter the vibrational modes of a carboxylate group (D1-Asp170) that is directly coordinated to the Mn ion that undergoes oxidation. In addition, it seems unlikely that replacing D1-Asp170 with the bulker His residue would have no appreciable affect on the wealth of spectral features that are observed in all of the mid-frequency S_{n+1}-*minus*-S_n FTIR difference spectra. Nevertheless, because mutations of D1-Glu189 [42] and D1-Asp342 [66] *also* produce no significant changes in the mid-frequency S_{n+1}-*minus*-S_n FTIR difference spectra (see Sections 2.3 and 2.7), the possibility that most Mn ligands are insensitive to the oxidations and structural changes that accompany the S state transitions is currently under active discussion (see Section 4).

2.3. Glutamate 189 of the D1 polypeptide

A principal disagreement between the X-ray crystallographic structural models and the earlier mutagenesis studies concerns the role of D1-Glu189. Both of the X-ray crystallographic structural models assign this residue as ligating the same Mn ion that is ligated by D1-His332 (*e.g.*, see Fig. 1). In contrast, the authors of the earlier mutagenesis studies concluded that D1-Glu189 does *not* ligate Mn. The reasons were that (1) D1-Glu189Gln, D1-Glu189Lys, and D1-Glu189Arg cells are photoautotrophic and evolve O_2 at 70–80% the rate of wild-type cells [67], (2) D1-Glu189Gln PSII particles exhibit normal S_1 and S_2 mutiline EPR signals [67], exhibit normal kinetics of O_2 release, and exhibit normal kinetics of electron transfer from Y_Z to $P_{680}^{\bullet+}$ and from the Mn_4Ca cluster to $Y_Z^{\bullet}$ during the $S_1 \rightarrow S_2$, $S_2 \rightarrow S_3$, and $S_3 \rightarrow S_0$ transitions [68], (3) D1-Glu189Lys and D1-Glu189Arg PSII particles exhibit normal rates of electron transfer from Y_Z to $P_{680}^{\bullet+}$ and from the Mn_4Ca cluster to $Y_Z^{\bullet}$ during the $S_1 \rightarrow S_2$ and $S_2 \rightarrow S_3$ transitions [68], and (4) D1-Glu189Asp, D1-Glu189Asn, D1-Glu189His, D1-Glu189Gly, and D1-Glu189Ser PSII particles contain Mn clusters that evolve no O_2, exhibit no S_1 or S_2 state multiline EPR signals, and are unable to advance beyond an altered $S_2Y_Z^{\bullet}$ state, as shown by the accumulation of narrow $S_2Y_Z^{\bullet}$ EPR signals under multiple turnover conditions [67]. Because changing D1-Glu189 to Gln, Lys, and Arg produced little change in PSII function, whereas changing D1-Glu189 to Asp, Asn, His, Gly, and Ser eliminated advancement beyond the $S_2Y_Z^{\bullet}$ state, it was proposed that D1-Glu189 participates in a network of hydrogen bonds that facilitates electron transfer from the Mn_4Ca cluster to $Y_Z^{\bullet}$ during the higher S state transitions [10,67,68]. This network is thought to be disrupted by inhibitory treatments that prevent advancement beyond the $S_2Y_Z^{\bullet}$ state (*e.g.*, the addition of acetate or ammonia or the depletion of Ca^{2+} or Cl^-) [54,69,70] and was proposed to be similarly disrupted in the non-O_2 evolving D1-Glu189 mutants [10,67]. It was proposed that this hydrogen bond network is maintained by Gln because of its hydrogen bonding characteristics and by Lys and Arg because of their flexibility and hydrogen bonding characteristics [10,67] and that this network compensates for the change in charge that is created when D1-Glu189 is changed to Gln, Lys, or Arg[6] [68].

In light of the recent X-ray crystallographic structural models, two groups employed FTIR difference spectroscopy to reassess whether D1-Glu189 ligates the Mn_4Ca cluster. In the first of these studies, the D1-Glu189Gln mutation was reported to cause small changes in the $\nu_{sym}(COO^-)$ region of the mid-frequency S_2-*minus*-S_1 FTIR difference spectrum and to cause larger changes between 640 cm^{-1} and 570 cm^{-1} in the low-frequency S_2-*minus*-S_1 FTIR difference spectrum [44]. The authors proposed that these spectral changes provided evidence for the ligation of Mn by D1-Glu189 [44]. However, the authors of a subsequent study presented evidence that the small differences between the mutant and wild-type spectra in the mid-frequency region arise from indirect mutation-induced structural perturbations rather than from the loss of a metal-ligating D1-Glu189 carboxylate group [42]. In this second study, the mutation-induced changes in both D1-Glu189Gln and D1-Glu189Arg PSII particles were shown to be similar in amplitude to those that are observed in (1) wild-type PSII particles that had been exchanged into FTIR analysis buffer by different methods and (2) D2-His189Gln PSII particles (D2-His189 interacts with Y_D [71,72] and is located >25 Å from the Mn_4Ca cluster [3,4]). It was concluded that the mid-frequency S_1-*minus*-S_0, S_2-*minus*-S_1, S_3-*minus*-S_2, and S_0-*minus*-S_3 FTIR difference spectra of D1-Glu189Gln and D1-Glu189Arg PSII particles are remarkably similar to those of wild-type PSII particles. Importantly, like the mutation D1-Asp170His, neither D1-Glu189 mutation eliminates any carboxylate modes from any of the difference spectra.

Regarding the low-frequency FTIR data, the spectral changes that were observed between 640 cm^{-1} and 570 cm^{-1} in the S_2-*minus*-S_1 FTIR difference spectrum of D1-Glu189Gln PSII particles [44] resemble the spectral changes that were observed previously in D1-Ala344stop and D1-Ala344Gly PSII particles [25,40] (see Section 2.1), D1-Asp170His PSII particles [43] (see Section 2.2), and in samples having Sr substituted for Ca [45] and have been attributed to indirect structural perturbations of

[6] To explain the photoautotrophic growth of the mutants D1-Glu189Leu and D1-Glu189Ile, it was proposed [67] that the relative bulk and hydrophobicity of Leu and Ile cause structural perturbations that permit the missing D1-Glu189 carboxylate group to be replaced by another residue, a peptide carbonyl, or a water molecule. As noted earlier, the same explanation was advanced previously [51] to account for the ability of D1-Asp170Val cells to grow photoautotrophically and the ability of D1-Asp170Leu and D1-Asp170Ile cells to evolve O_2 despite the apparent role of D1-Asp170 as a ligand to Mn.

a single Mn–O–Mn cluster mode [42,43,45,46]. Consequently, the D1-Glu189Gln mutation-induced spectral changes that are observed between 640 cm^{-1} and 570 cm^{-1} likely have the same origin.

One explanation for the similarity of the mid-frequency FTIR difference spectra of D1-Glu189Gln, D1-Glu189Arg, and wild-type PSII particles is that, as proposed for D1-Asp170 [46], D1-Glu189 ligates a Mn ion that does not change its charge or formal oxidation state during the $S_0 \rightarrow S_1$, $S_1 \rightarrow S_2$, or $S_2 \rightarrow S_3$ transitions. However, ligation of Mn by D1-Glu189 is difficult to reconcile with the earlier analyses of D1-Glu189 mutants (described above). An alternate explanation for the FTIR data is that D1-Glu189 does *not* ligate a Mn ion. This conclusion would be consistent with the earlier mutagenesis studies, but requires that the proximity of D1-Glu189 to Mn in the recent X-ray crystallographic structural models [3,4] be an artifact of the radiation-induced reduction of the cluster's Mn(III) and Mn(IV) ions that occurred during the collection of the X-ray diffraction data.

In both recent X-ray crystallographic structural models (*e.g.*, see Fig. 1), D1-Glu189 residue is either located near to [3] or identified as a possible ligand of [4] the Ca ion. Coordination of Ca by D1-Glu189 would be consistent with both the FTIR data and the earlier mutagenesis studies if replacing D1-Glu189 with other residues weakens the affinity of Ca for PSII to the extent that, in mutants other than D1-Glu189Gln, D1-Glu189Lys, and D1-Glu189Arg, the network of hydrogen bonds that facilitates electron transfer from Mn to $Y_Z^\bullet$ is disrupted sufficiently to prevent advancement beyond the $S_2Y_Z^\bullet$ state [42]. The Ca ion is believed to form part of this network [73,74] and its ligation by D1-Glu189 was proposed previously on the basis of spectroscopic analyses of Ca-depleted PSII preparations [73]. It has been observed that D1-Glu189Gln cells do not grow photoautotrophically in media having Sr substituted for Ca (R. J. D., unpublished).

2.4. Histidine 332 of the D1 polypeptide

In both X-ray crystallographic structural models of PSII, D1-His332 ligates the same Mn ion as D1-Glu189 [3,4] (*e.g.*, see Fig. 1). Ligation of Mn by at least one histidine residue was demonstrated earlier by a 9 GHz ESEEM study that examined PSII preparations that had been labeled with [^{15}N]histidine [75]. Recent 31 and 34 GHz ESEEM studies of unlabeled and globally ^{15}N-labeled samples support Mn ligation by a single histidine residue [76]. Other 9 GHz ESEEM studies have provided evidence that the ligating histidine residue coordinates Mn with its $\varepsilon 2$ (τ) nitrogen [77] and that the ligating histidine residue is D1-His332 [78] (see below). Additional evidence for the coordination of Mn by histidine has been provided by FTIR studies conducted with [^{15}N]histidine [79,80]. These studies show that histidine vibrational modes between 1120 and 1099 are altered during the $S_0 \rightarrow S_1$ transition [80] and are restored during the $S_1 \rightarrow S_2$ [79,80] and $S_2 \rightarrow S_3$ transitions [80], but do not change during the $S_3 \rightarrow S_0$ transition [80]. The earlier FTIR study provided additional evidence that the ligating histidine coordinates Mn with its $\varepsilon 2$ (τ) nitrogen, and that its $\delta 1$ (π) nitrogen is protonated and participates in a hydrogen bond [79]. In both X-ray crystallographic structural models [3,4], the $\delta 1$ (π) nitrogen of D1-His332 is located within hydrogen-bonding distance of the peptide carbonyl of D1-Glu329.

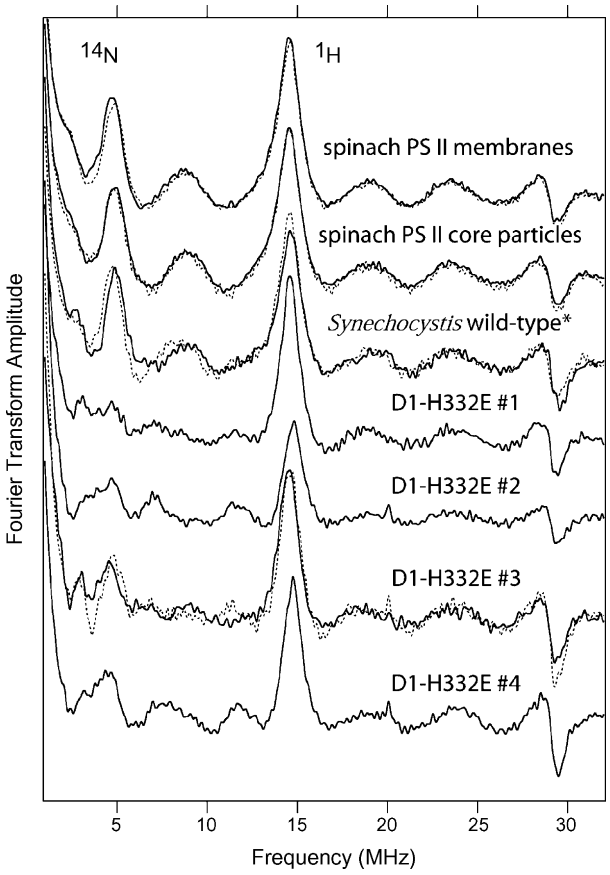

Fig. 7. Fourier transforms of normalized two-pulse time domain light-*minus*-dark ESEEM patterns of the S_2 state multiline EPR signal of spinach PSII membranes, spinach PSII core particles, *Synechocystis* wild-type PSII particles, and four independent preparations of *Synechocystis* D1-His332Glu PSII particles (preparations #1 to #4). For the spinach PSII membranes, the solid and dashed lines correspond to independent preparations that were illuminated at different temperatures. For the spinach PSII core and *Synechocystis* wild-type PSII particles, the solid and dashed lines correspond to independent sample preparations. For D1-His332Glu PSII preparation #3, the dashed line corresponds to an independent aliquot of the same sample. In the spectrum of the wild-type PSII particles, the ~4.8 MHz feature corresponds to nitrogen modulation from a histidyl Mn ligand of the Mn_4Ca cluster. Note that the amplitude of this feature is sharply diminished in D1-His332Glu PSII particles, consistent with the Mn ligation by D1-His332. The features at ~14.5 GHz and ~29 GHz correspond to protons that are weakly coupled to the electron spin of the Mn tetramer (modified from Ref. [78], reprinted with permission, copyright 2001 by the American Chemical Society).

Ligation of Mn by D1-His332 was proposed originally on the basis of site-directed mutagenesis studies of several D1-His332 mutants [81,82]. To test this proposal, a 9 GHz ESEEM study of D1-His332Glu PSII particles was conducted [78]. This study showed that the nitrogen modulation that is observed near 5 MHz in the two-pulse ESEEM spectrum of the S_2 state multiline EPR signal of wild-type PSII particles is diminished substantially in D1-His332Glu PSII particles (Fig. 7) [78]. Because this modulation arises from magnetic coupling between the Mn ions of

the Mn_4Ca cluster and a histidyl ligand [75], the diminished amplitude of this modulation in D1-His332Glu PSII particles provides strong spectroscopic evidence that D1-His332 ligates Mn [78]. The diminished nitrogen modulation amplitude could represent either the loss of the ligating D1-His332 $\varepsilon 2$ (τ) nitrogen, decreasing the coordination number of one Mn ion from six to five, or the replacement of the ligating nitrogen with an oxygen from glutamate or with an oxygen from another residue, peptide group, or water molecule [78].

Of the many D1-His332 mutants that have been constructed in *Synechocystis* 6803 [9,81–83], none are photoautotrophic and only the D1-His332Gln and D1-His332Ser mutants evolve O_2, and these at only 10–15% the rate of wild-type cells. On the basis of Chl *a* fluorescence analyses that were conducted with intact cells, it was concluded only 20–40% of the PSII reaction centers in most D1-His332 mutants assemble photooxidable Mn clusters [82]. The exceptions were D1-His332Asp and D1-His332Glu. Essentially all of the PSII reaction centers in these mutants contain photooxidizable Mn clusters. Intact D1-His332Glu PSII particles exhibit an altered S_2 state multiline EPR signal that has more hyperfine lines and narrower splittings than the S_2 state multiline EPR signal that is observed in wild-type PSII preparations [78,84]. However, the quantum yield for oxidizing the S_1 state Mn cluster in D1-His332Glu cells [83] and PSII particles [84] is very low, corresponding to a 350-fold [83] or 8000-fold [84] slowing of the rate of electron transfer from the Mn cluster to $Y_Z^{\bullet}$. This rate is also slowed in many other D1-His332 mutants, including D1-His332Lys and D1-His332Asp [82,83]. The temperature threshold for forming the S_2 state has been measured to be approximately 100 K higher in D1-His332Glu PSII particles than in wild-type PSII particles [84] and to be substantially higher in both D1-His332Asp and D1-His332Glu cells than in wild-type cells [83], but to be essentially unchanged in D1-His332Ser cells [83]. The accumulation of a narrow $S_2Y_Z^{\bullet}$ EPR signal under multiple turnover conditions shows that the Mn clusters in D1-His332Glu PSII particles are unable to advance beyond an altered $S_2Y_Z^{\bullet}$ state [84]. Complete blockage or a substantial slowing of the S_2–S_3 transition is believed to be characteristic of the Mn clusters in numerous other D1-His332 mutants [82,83]. The kinetics of charge recombination between $Q_A^{\bullet -}$ and the S_2 state and between $Q_A^{\bullet -}$ and $Y_Z^{\bullet}$ are also altered in most D1-His332 mutants, showing that these mutations alter the midpoint potentials of both S_2/S_1 and $Y_Z^{\bullet}/Y_Z$, resulting in a stabilization of the S_2 state compared to wild-type [83,84].

These results described in the previous paragraph are consistent with D1-His332 both ligating Mn and participating in a network of hydrogen bonds that facilitates proton-coupled electron transfer from Mn to $Y_Z^{\bullet}$ during the higher S state transitions [78,83,84]. This network presumably involves D1-Glu329 (see above) [3,4] and has been proposed to be similarly disrupted in the non-photoautotrophic D1-Glu189 mutants [10,67] (see Section 2.3) and in most D1-His332 mutants [78,83,84].

As noted in Section 2.2, D1-Asp170 provides part of the high-affinity binding site for the first Mn(II) ion that is photooxidized during the light-driven assembly of the Mn_4Ca cluster [47–49]. Mutations of D1-His332 slightly decrease the affinity of Mn(II) ions for this site, as do mutations at other C-terminal residues of the D1 polypeptide such as D1-Glu333, D1-Asp342, and D1-Ala344 (see Sections 2.1, 2.5 and 2.6) [39]. As noted earlier, this lowered affinity implies that the C-terminal region of the D1 polypeptide is located near D1-Asp170 in the apo-protein and suggests that this region either increases the local concentration of Mn(II) ions near the D1-Asp170 high-affinity site or stabilizes a conformation that optimizes the affinity of this site for Mn(II) ions [39].

The PSII reaction centers in D1-His332 mutants appear to have substantially diminished affinities for Ca [82]. When these mutants are propagated photoheterotrophically in media containing Na substituted for Ca, the rate of electron transfer from Y_Z to $P_{680}^{\bullet +}$ appears to slow dramatically, as is observed in PSII preparations that have been rigorously depleted of Ca ions [85,86]. This lowered affinity of PSII for Ca ions appears to be a general feature of C-terminal mutants, such as those constructed at D1-Glu333, D1-His337, and D1-Asp342 (see Sections 2.5–2.7) [82]. Because the X-ray crystallographic structural models place the Ca ion on the opposite side of the Mn_4Ca cluster from the C-terminal region of the D1 polypeptide [3,4], it is likely that mutations in this region alter the protein conformation around the Mn_4Ca cluster sufficiently to influence the binding of Ca.

Several His332 mutants are extremely susceptible to light-induced damage [82]. This damage is reflected as both low cellular PSII contents and substantially altered charge recombination kinetics between $Q_A^{\bullet -}$ and the Mn cluster in cells propagated in normal *versus* dim light. Because cells that are unable to assemble Mn clusters *in vivo* (*e.g.*, cells of the mutants D1-Asp170Ala, D1-Asp170Thr, D1-Asp170Ser, and D1-Asp170Asn) are *not* particularly light-sensitive [51], it has been proposed that the extreme light-sensitivity of the light-sensitive His332 mutants is caused by the release of toxic, activated oxygen species from perturbed Mn clusters [82]. This extreme sensitivity to light-induced damage appears to be a general feature of C-terminal mutants, such as those constructed at D1-Glu333, D1-His337, and D1-Asp342 (see Sections 2.5–2.7) [82].

2.5. Glutamate 333 of the D1 polypeptide

In both X-ray crystallographic structural models of PSII, D1-Glu333 ligates the same Mn ion as D1-Asp170, either as a unidentate ligand [3] or as a bridging ligand that links this Mn ion with a Mn ion that is ligated by Glu354 of the CP43 polypeptide [4] (Fig. 1). No FTIR studies of D1-Glu333 mutants have yet been published. Of the D1-Glu333 mutants that have been reported (Gln, Asp, Asn, His, Cys, Ala, and Tyr), only D1-Glu333Gln cells are photoautotrophic or evolve O_2, but these cells evolve O_2 at only 29–36% the rate of wild-type cells [39,81,82]. In all of the D1-Glu333 mutants, substantial percentages of PSII reaction centers lack photooxidizable Mn ions *in vivo* [82]. These percentages range from ~25% and ~40% in D1-Glu333Gln and D1-Glu333Asp cells, respectively, to ~60% in D1-Glu333Tyr cells. On the basis of these observations, D1-Glu333 was identified as a possible ligand of Mn [81,82].

All D1-Glu333 mutants, like several D1-His332 mutants, are extremely susceptible to light-induced damage [82]. As with the light-sensitive D1-His332 mutants, it was proposed that the extreme light-sensitivity of the light-sensitive Glu333 mutants is caused by the release of toxic, activated oxygen species from perturbed Mn clusters [82]. On the basis of Chl *a* fluorescence analyses that were conducted with intact cells that were propagated in dim light, it was concluded that the apparent S_2/S_1 midpoint potential is essentially unchanged in D1-Glu333Gln and D1-Glu333Asp cells, but is slightly decreased in D1-Glu333Asn and D1-Glu333His cells [82].

Mutations of D1-Glu333 decrease the affinity of Mn(II) ions for the high-affinity D1-Asp170 site similarly to mutations at other C-terminal residues of the D1 polypeptide such as D1-His332, D1-Asp342, and D1-Ala344 (see Sections 2.1, 2.4 and 2.7) [39], again suggesting that this region either increases the local concentration of Mn(II) ions near the high-affinity site or stabilizes a conformation that optimizes the affinity of this site for Mn(II) ions [39]. The PSII reaction centers in D1-Glu333 mutant cells appear to have substantially diminished affinities for Ca, like those in D1-His332 cells [82]. As noted earlier, this lowered affinity of PSII for Ca ions appears to be a general feature of many C-terminal mutants (see Sections 2.3, 2.4, 2.6 and 2.7) [82].

2.6. Histidine 337 of the D1 polypeptide

Both recent X-ray crystallographic structural models place D1-His337 close to the Mn_4Ca cluster, but ligating neither Mn nor Ca [3,4] (*e.g.*, see Fig. 1). Of the nine mutants that have been reported [81,82], only the Arg, Gln, Asn, and Phe mutants are photoautotrophic, although the Gln, Asn, and Phe mutants are only weakly so. In all of the His337 mutants, 10–50% of PSII reaction centers lack photooxidizable Mn ions *in vivo* [82]. On the basis of these observations, D1-His337 was identified as a possible ligand of Mn [82]. On the other hand, because Arg and Gln are good hydrogen bond donors that can substitute for His (*e.g.*, Gln replaces His as a hydrogen bond donor in nitrogenase from *Azotobacter vinelandii* [87,88], in sperm whale myoglobin [89], and in ribulose-1,5-bisphosphate carboxylase/oxygenase from *Anacystis nidulans* [90]), D1-His337 was also suggested to serve as a crucial hydrogen bond donor whose influence on the Mn_4Ca cluster is indirect [82]. No spectroscopic studies have yet been reported on any D1-His337 mutant.

The Mn clusters in D1-His337Val cells are severely perturbed, whereas those in D1-His337Leu cells evolve O_2, and those in D1-His337Phe cells support photoautotrophic growth [82]. To explain this curious observation, that progressively larger hydrophobic residues cause progressively less functional damage, the bulky Leu and Phe residues were proposed to cause structural perturbations that permit the missing imidazole moiety of D1-His337 to be replaced by another residue, a peptide carbonyl group, or a water molecule [82]. As noted earlier (Sections 2.2 and 2.3), similar explanations were proposed to rationalize the photoautotrophic growth of D1-Asp170Val and D1-Glu189Leu cells despite the apparent role of D1-Asp170 as a ligand to Mn and the apparent role of D1-Glu189 as a participant in a critical hydrogen bond network or as a ligand to Mn [51,67].

Like mutants of other C-terminal residues (*e.g.*, D1-His332, D1-Glu333, D1-Asp342, D1-Ala344), mutants of D1-His337 decrease the affinity of PSII for Ca [82]. Many are also extremely susceptible to the light-induced damage that was attributed to the release of toxic, activated oxygen species from perturbed Mn clusters in other C-terminal mutants [82] (see Sections 2.1 and 2.3–2.5).

2.7. Aspartate 342 of the D1 polypeptide

Of the five mutations that have been reported [81,82], only D1-Asp342Glu supports photoautotrophic growth and only D1-Asp342Glu, D1-Asp342Asn, and D1-Asp342His support O_2 evolution, and at only ~20%, ~33%, and ~6% the rate of wild-type cells, respectively. Because 20–50% of the PSII reaction centers in the D1-Asp342 mutants lack photooxidizable Mn ions [82], and because O_2 evolution is retained when D1-Asp342 is replaced with a potential metal ligand (*e.g.*, Glu, Asn, or His) but not when replaced by Ala or Val, this residue was identified as a possible ligand of Mn [81,82]. This proposal is supported by the recent X-ray crystallographic structural models that assign D1-Asp342 as a unidentate ligand of a single Mn ion [3] or as a bridging ligand between two Mn ions [4] (Fig. 1).

The mid-frequency (1800–1200 cm^{-1}) FTIR difference spectra of the $S_0 \rightarrow S_1$, $S_1 \rightarrow S_2$, or $S_2 \rightarrow S_3$ transitions in D1-D342N PSII particles closely resemble the corresponding spectra of wild-type PSII particles [66]. In particular, the data provide no indication that the mutation eliminates a specific carboxylate vibrational mode from any of the S_{n+1}-*minus*-S_1 FTIR difference spectra. These observations show that, like D1-Asp170 and D1-Glu189, D1-Asp342 is insensitive to the oxidations of the Mn_4Ca cluster that occur during the $S_0 \rightarrow S_1$, $S_1 \rightarrow S_2$, or $S_2 \rightarrow S_3$ transitions. The simplest explanation for these data is that D1-Asp342 ligates a Mn ion that does not increase its charge or oxidation state during any of these S state transitions [66]. Because the same conclusion was reached previously for D1-Asp170 [46] (Section 2.2) and D1-Glu189 [42] (Section 2.3), and because the X-ray crystallographic structural models assign D1-Asp170 and D1-Asp342 as ligating different Mn ions (*e.g.*, see Fig. 1), this explanation requires that (1) the extra positive charge that develops on the Mn cluster during the $S_1 \rightarrow S_2$ transition be localized on the Mn ion that is ligated by the α-COO^- group of D1-Ala344 and (2) any increase in positive charge that develops on the Mn cluster during the $S_0 \rightarrow S_1$ and $S_2 \rightarrow S_3$ transitions be localized on the one Mn ion that is *not* ligated by D1-Asp170, D1-Glu189, D1-Asp342, or D1-Ala344 (however, see Section 4). Additional experiments that were conducted with L-[1-^{13}C]alanine provided evidence that D1-Asp342 does not ligate the same Mn ion that is ligated by the α-COO^- group of D1-Ala344 [66].

The D1-Asp342 mutations slightly decrease the affinity of Mn(II) ions for the high-affinity Mn site formed by D1-Asp170 [39] and appear to substantially diminish the affinity of PSII for Ca [82], similarly to mutations constructed at other C-terminal residues of the D1 polypeptide such as D1-His332,

D1-Glu333, D1-His337, and D1-Ala344 (see Sections 2.1 and 2.3–2.5). Some D1-Asp342 mutants, like several D1-His332 mutants, all D1-Glu333 mutants, and some D1-His337 mutants, are extremely susceptible to light-induced damage [82]. As with the other light-sensitive C-terminal mutants, it was proposed that the extreme light-sensitivity of the light-sensitive D1-Asp342 mutants is caused by the release of toxic, activated oxygen species from perturbed Mn clusters [82].

2.8. Glutamate 354 of the CP43 polypeptide[7]

In the recent X-ray crystallographic structural models of photosystem II, Glu354 of the CP43 polypeptide is assigned as either a bidentate chelating ligand of a single Mn ion that has no other protein ligands [3] or as a bridging ligand between one Mn ion that is ligated by D1-Glu333 and another Mn ion that is ligated by the α-COO^- group of D1-Ala344 [4] (*e.g.*, see Fig. 1). Only the CP43-Glu354Gln mutant has been reported [92,93]. This mutant is weakly photoautotrophic. The steady-state rate of O_2 evolution in the mutant cells is only about 20% compared to wild-type [92,93], but the kinetics of O_2 release are essentially unchanged and the O_2 flash yields show normal period-four oscillations, although with lower intensities after each flash [93]. Purified PSII particles exhibit an essentially normal S_2 state multiline EPR signal, but exhibit a substantially altered S_2-*minus*-S_1 FTIR difference spectrum [93]. The intensities of the mutant EPR and FTIR difference spectra (>75% compared to wild-type) are much greater than the O_2 signals and suggest that CP43-Glu354Gln PSII reaction centers are heterogeneous, with a minority fraction able to evolve O_2 with normal O_2 release kinetics and a majority fraction unable to advance beyond the S_2 or S_3 states.

The S_2-*minus*-S_1 FTIR difference spectrum of CP43-Glu354Gln PSII particles is altered in both the symmetric and asymmetric carboxylate stretching regions [93] (Fig. 8). One of the most dramatic alterations is the complete elimination of the positive band at 1588 cm^{-1}. Although this band may correspond to the $\nu_{asym}(COO^-)$ mode of CP43-Glu354, because the $\nu_{asym}(COO^-)$ region overlaps the amide I and amide II regions, some of the observed spectral alterations in the $\nu_{asym}(COO^-)$ region undoubtedly arise from mutation-induced perturbations to the polypeptide backbone. Preliminary global ^{15}N-labeling experiments conducted with both wild-type and CP43-Glu354Gln PSII particles (M.A. Strickler, R.J. Debus, unpublished) indicate that the positive band at 1588 cm^{-1} band corresponds to a $\nu_{asym}(COO^-)$ mode, in agreement with earlier global ^{15}N-labeling studies [94–96]. However, these same experiments confirm that the mutation alters numerous amide I and amide II modes, raising the possibility that structural perturbations introduced by the mutation and/or the loss of the negative charge on CP43-Glu354 might change the distribution of Mn oxidation states within the Mn_4Ca cluster and cause a different Mn ion to undergo oxidation during the $S_1 \rightarrow S_2$ transition. Indeed, preliminary [1-^{13}C]alanine-labeling experiments that were conducted with both wild-type and CP43-Glu354Gln PSII particles (M.A. Strickler, R.J. Debus, unpublished) indicate that the Mn ion that is ligated by the α-COO^- group of D1-Ala344 does *not* undergo oxidation during the $S_1 \rightarrow S_2$ transition in the mutant. These experiments probably account for the negative band at 1351 cm^{-1} and the positive band at 1334 cm^{-1} that appear in the WT-*minus*-mutant double-difference spectrum (Fig. 8, lower trace).

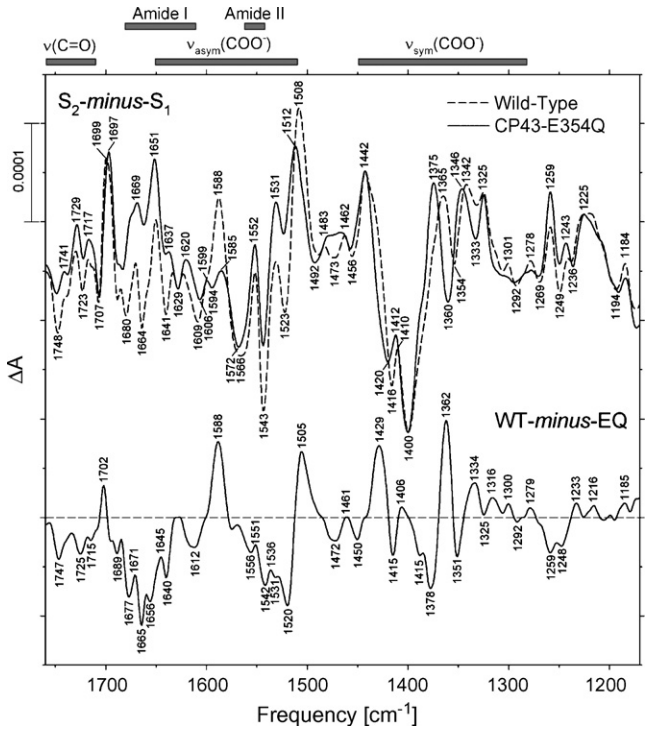

Fig. 8. Comparison of the mid-frequency S_2-*minus*-S_1 FTIR difference spectra (upper traces) of wild-type (dashed) and CP43-Glu354Gln (solid) PSII particles. The wild-type spectrum represents the average of 10,800 scans. The CP43-Glu354Gln spectrum represents an average of 31,500 scans. The spectra have been normalized to maximize overlap. A wild-type-*minus*-mutant double difference spectrum (lower trace) was calculated by directly subtracting the S_2-*minus*-S_1 FTIR difference spectra shown in the upper traces. The horizontal dashed line indicates the zero level (reprinted from Ref. [93]).

Although the $\nu_{asym}(COO^-)$ and/or $\nu_{asym}(COO^-)$ modes of CP43-Glu354 may be present in the S_2-*minus*-S_1 FTIR difference spectrum of wild-type PSII particles (and absent from the spectrum of CP43-Glu354Gln PSII particles), the large number of features in the WT-*minus*-mutant double-difference spectrum (Fig. 8, lower trace) precludes any definite assignment. Furthermore, if the CP43-Glu354Gln mutation changes the distribution of Mn oxidation states in the Mn_4Ca cluster and induces a different Mn ion to undergo oxidation during the $S_1 \rightarrow S_2$ transition, then many of the features that differ between the wild-type and mutant S_2-*minus*-S_1 FTIR difference spectra may correspond to the $\nu_{asym}(COO^-)$ or $\nu_{asym}(COO^-)$ modes of carboxylate groups other than CP43-Glu354. Without the examination of

[7] Multiple numbering systems are in use for the CP43 polypeptide because *psbC* (the gene encoding CP43) has an unusual start codon, because CP43 is post-translationally processed at its amino terminus, and because, in *Synechocystis* sp. PCC 6803, there is a deletion of one residue at position 7 compared to the amino acid sequences of CP43 in other organisms [11,91]. The numbering system used in the X-ray crystallographic structural models [3,4] is used here.

additional mutants, we cannot be sure if *any* of the features in the S_2-*minus*-S_1 FTIR difference spectrum of wild-type PSII particles correspond to the $\nu_{sym}(COO^-)$ or $\nu_{asym}(COO^-)$ modes of CP43-Glu354.

One aspect of the CP43-Glu354Gln S_2-*minus*-S_1 FTIR difference spectrum is clear: a large positive band at 1588 cm^{-1} is eliminated, yet the negative band at 1400 cm^{-1} is unchanged (Fig. 8). This observation is difficult to reconcile with an assignment of these two modes to a single Mn–Mn or Mn–Ca bridging carboxylate group that has its $\nu_{asym}(COO^-)$ mode at ~1587 cm^{-1} in the S_2 state and its $\nu_{sym}(COO^-)$ mode at ~1403 cm^{-1} in the S_1 state. This assignment has been proposed on the basis of analyses of Ca-depleted PSII preparations [94,97]. However, the S_2-*minus*-S_1 FTIR difference spectrum is altered far more substantially by Ca-depletion [94,97] than by the CP43-Glu354Gln mutation [93] (Fig. 8). Consequently, substantially more amino acid residues in the environment of the Mn_4Ca cluster must be perturbed by the depletion of Ca than by the CP43-Glu354Gln mutation. Because the CP43-Glu354Gln mutation eliminates the positive 1588 cm^{-1} band but not the negative 1400 cm^{-1} band, these two bands must correspond to different carboxylate groups.

3. Protein ligation of calcium

In the 3.5 Å crystallographic structural model [3], the Ca ion has no protein ligands. In the 3.0 Å crystallographic structural model [4] (Fig. 1), the Ca ion interacts weakly with D1-Glu189 and D1-Ala344 (with Ca–O distances of 2.5 Å and 2.6 Å, respectively), both of which interact much more strongly with Mn1 and Mn2, respectively (the Mn–O distances are 1.8 Å and 1.7 Å, respectively). A Ca site having no protein ligands would be highly unusual in that such sites typically contain oxygen atoms from peptide carbonyl groups and the side chains of Asp, Glu, Asn, or Gln in addition to those provided by water molecules [98,99]. On the basis of the earlier mutagenesis studies, both D1-Asp59 and D1-Asp61 were suggested as possible Ca ligands [51], while D1-Asp342 was suggested as a possible ligand of Mn or Ca or both [82]. In the mutagenesis studies, D1-Asp59 was changed to Glu, Asn, and Val, while D1-Asp61 was changed to Glu, Asn, Ala, and Val [51,81]. The D1-Asp59Glu, D1-Asp59Asn, and D1-Asp61Glu mutants are strongly photoautotrophic, whereas the others are weakly so. The D1-Asp59Asn and D1-Asp61Glu mutants exhibit O_2 flash-yields that have normal period-four oscillations [100]. The D1-Asp59Asn, D1-Asp61Asn, and D1-Asp61Ala mutants evolve O_2 at only 20–30% the rate of wild-type cells and the D1-Asp59Val and D1-Asp61Val mutants are even more impaired. On the basis of Chl *a* fluorescence analyses that were conducted with intact cells, it was concluded that essentially all of the PSII reaction centers in the D1-Asp59 and D1-Asp61 mutants contain intact, photooxidizable Mn clusters *in vivo* [51]. Therefore, it was concluded that neither D1-Asp59 nor D1-Asp61 was likely to ligate Mn. Nevertheless, at least one unstable intermediate in the light-driven assembly (photoactivation) of the Mn_4Ca cluster is destabilized dramatically in both D1-Asp59Asn and D1-Asp61Glu cells [100].

The rate of O_2 release is slowed dramatically in D1-Asp61Asn and D1-Asp61Ala cells (10-fold in D1-Asp61Asn cells and eightfold in D1-Asp61Ala cells) [101] and is slowed to lesser extents in D1-Asp61Glu and D1-Asp59Asn thylakoid membranes [100]. Subsequent analyses showed that the $S_1 \rightarrow S_2$ and $S_2 \rightarrow S_3$ transitions are slowed approximately twofold in D1-Asp61Asn PSII particles [101] and that the $S_3 \rightarrow S_0$ transition is slowed 10-fold [102], consistent with the very slow kinetics of O_2 release in this mutant.

Both D1-Asp59 and D1-Asp61 were identified as possible ligands to Ca in the mutagenesis studies because the PSII reaction centers in D1-Asp59Asn and D1-Asp61Ala cells exhibit substantially diminished affinities for Ca. Neither mutant grew photoautotrophically when Ca was omitted from the growth medium: neither Sr, Mg, nor Na would substitute [51]. In addition, when D1-Asp59Asn and D1-Asp61Ala cells were propagated photoheterotrophically in the absence of Ca, little or no O_2 evolution was observed, the rate of electron transfer from Y_Z to $P_{680}^{\bullet+}$ slowed dramatically (as is observed in PSII preparations that have been rigorously depleted of Ca ions [85,86]), and PSII became very susceptible to light-induced damage [51]. Because neither residue is located near Ca in the X-ray crystallographic structural models [3,4] (*e.g.*, see Fig. 1), the D1-Asp59Asn and D1-Asp61Ala mutations evidently weaken the affinity of PSII for Ca by causing indirect structural perturbations. Presumably such indirect structural perturbations also explain the lowered affinity of PSII for Ca in mutants of D1-Arg64 [103] and, as noted earlier, in mutants constructed at D1-His332, D1-Glu333, D1-His337, and D1-Asp342 [82] (see Sections 2.4–2.7). The dramatically slower rates of O_2 release in the D1-Asp61Asn and D1-Asp61Ala mutants may be caused by the inability of Asn or Ala to replace D1-Asp61 in the latter's postulated role as the initial residue in a proton transfer pathway that leads from the Mn4Ca cluster to the thylakoid lumen [3,104,105].

4. Concluding remarks and perspectives

The emerging availability of high-resolution X-ray crystallographic structural models for PSII is dramatically improving the power of spectroscopy to provide mechanistic insight into the operation of the oxygen-evolving complex. The current ~3.0 Å and ~3.5 Å models [3,4] (Fig. 1) are already serving as valuable guides for spectroscopic studies designed to elucidate the roles of specific amino acid residues. Many of these studies involve FTIR difference spectroscopy. To date, FTIR studies have provided strong evidence that the α-COO^- group of D1-Ala344 is a unidentate ligand of a Mn ion whose charge or formal oxidation state increases during the $S_1 \rightarrow S_2$ transition and that the carboxylate groups of D1-Asp170, D1-Glu189, and D1-Asp342 are sensitive to neither the Mn oxidations nor the structural changes that accompany the $S_0 \rightarrow S_1$, $S_1 \rightarrow S_2$, and $S_2 \rightarrow S_3$ transitions.

However, the FTIR studies have produced an apparent paradox. The individual S_{n+1}-*minus*-S_n FTIR difference spectra of wild-type PSII preparations contain a wealth of spectral features in the mid-frequency region (*e.g.*, see Figs. 2 and 6). It has long been assumed that most of these features, particularly those

corresponding to carboxylate stretching modes, would arise from amino acid residues that ligate the Mn_4Ca cluster. However, half of the carboxylate residues identified as metal ligands in the X-ray crystallographic structural models are insensitive to the oxidations and structural changes that accompany the $S_0 \rightarrow S_1$, $S_1 \rightarrow S_2$, and $S_2 \rightarrow S_3$ transitions (i.e., D1-Asp170, D1-Glu189, and D1-Asp342). Two explanations for this apparent paradox have been presented. Each has its difficulties.

One explanation is that the charge that develops on the Mn_4Ca cluster during the $S_1 \rightarrow S_2$ transition is localized on the Mn ion that is ligated by the α-COO^- group of D1-Ala344 and that any increase in positive charge that develops on the Mn cluster during the $S_0 \rightarrow S_1$ and $S_2 \rightarrow S_3$ transitions is localized on the *one* Mn ion that is *not* ligated by D1-Asp170, D1-Asp342, or D1-Ala344 (or D1-Glu189, if this residue ligates Mn). In both X-ray crystallographic models, this Mn corresponds to Mn3, the Mn ion that is ligated by CP43-Glu354 in the ∼3.5 Å structural model [3] and by both CP43-Glu354 and D1-Glu333 in the ∼3.0 Å structural model [4] (Fig. 1). Difficulties with this explanation are (1) it conflicts with an inelastic X-ray scattering (RIXS) study whose authors concluded that the electron that leaves the Mn_4Ca cluster during the $S_1 \rightarrow S_2$ transition originates from a strongly delocalized orbital [106], implying that the extra charge that develops on the Mn_4Ca cluster during this transition must be delocalized over multiple Mn ions, (2) if the $S_2 \rightarrow S_3$ transition corresponds to a metal-centered oxidation [64,107], then this explanation would be difficult to reconcile with an oxidation state distribution of $Mn(III)_3Mn(IV)$ for the S_0 state as proposed on the basis of a recent ^{55}Mn pulsed ENDOR study [108] (with this oxidation state distribution, different Mn ions would necessarily undergo oxidation during each of the $S_0 \rightarrow S_1$, $S_1 \rightarrow S_2$, and $S_2 \rightarrow S_3$ transitions), (3) it seems odd that the structural changes that accompany the $S_0 \rightarrow S_1$ and $S_2 \rightarrow S_3$ transitions [63–65] would perturb the carboxylate groups of neither D1-Asp170, nor D1-Glu189, nor D1-Asp342, and (4) there appear to be more features in the carboxylate stretching regions of the S_{n+1}-*minus*-S_n FTIR difference spectra than can be accounted for if none arises from D1-Asp170, D1-Glu189, or D1-Asp342. Nevertheless, no FTIR study of any D1-Glu333 mutant has yet appeared, the mid-frequency S_2-*minus*-S_1 FTIR difference spectrum of CP43-Glu354Gln PSII particles shows numerous mutation-induced alterations [93], XANES data have been interpreted in terms of an oxidation state distribution of $Mn(II)Mn(III)Mn(IV)_2$ for the S_0 state [109,110], and whether the $S_2 \rightarrow S_3$ transition corresponds to a metal-centered [64,107] or ligand-centered [109,110] oxidation remains in dispute.

A second explanation is that the carboxylate stretching modes of the carboxylate ligands of the Mn_4Ca cluster are mostly insensitive to changes in the formal oxidation states of the individual Mn ions [35,58]. This situation might arise if the Mn oxidations that occur during the S state transitions cause little increase in the electrostatic charge of the individual Mn ions, a prediction that was obtained from a QM/MM analysis of the ∼3.5 Å X-ray crystallographic structural model [35]. This situation might also arise if most of the Mn_4Ca cluster's Mn-ligating carboxylate ligands bind as equatorial ligands. Perhaps the α-COO^- group of D1-Ala344 ligates along the Jahn-Teller axis of a Mn(III) ion. If so, then the ∼16 cm^{-1} or ∼34 cm^{-1} downshift of this group's symmetric carboxylate stretching mode during the $S_1 \rightarrow S_2$ transition [24,25] might arise from the shortening of an elongated Mn–O bond that would occur when this Mn(III) ion is oxidized to its Mn(IV) oxidation state.[8] These explanations would account for the observed insensitivity of D1-Asp170 [43,46], D1-Glu189 [42], and D1-Asp342 [66] to oxidations of the Mn_4Ca cluster during the $S_0 \rightarrow S_1$, $S_1 \rightarrow S_2$, or $S_2 \rightarrow S_3$ transitions. However, they do not account for the strikingly large number of features that are present in the individual S_{n+1}-*minus*-S_n FTIR difference spectra, many of which correspond to perturbations of symmetric and asymmetric modes of carboxylate groups in response to oxidations of the Mn_4Ca cluster. It should be noted that these perturbations are unlikely to correspond to changes in the protonation states of free carboxylate groups. Protonated carboxylate residues show a carbonyl stretching mode [ν(C=O)] at 1760–1710 cm^{-1} [111]. If the pK_a value of a carboxylate residue changed during a particular S state transition, the intensities of its ν(C=O) and $\nu_{sym}(COO^-)$/$\nu_{asym}(COO^-)$ modes would change in inverse correlation as one form of the residue converted into the other. Because the features in the ν(C=O) regions of the S_{n+1}-*minus*-S_n FTIR difference spectra of wild-type PSII preparations are much weaker than those in the $\nu_{sym}(COO^-)$ and $\nu_{asym}(COO^-)$ regions, it is unlikely that the features in these two regions correspond to the same amino acid residues.

Differentiating between these explanations will require the examination of additional mutants, especially of residues located farther from the Mn_4Ca cluster than its protein ligands, will require the examination of relevant and well-characterized inorganic model compounds (*e.g.*, [112–114]), and will require further extension of FTIR studies to the low-frequency domain (1000–350 cm^{-1}) where Mn–O and Mn–N vibrational modes appear [19–22].

Acknowledgements

The author is grateful to Warwick Hillier, Gary W. Brudvig, Victor S. Batista, David F. Bocian, and Takumi Noguchi for many stimulating discussions and to Warwick Hillier, Gary W. Brudvig, and the reviewers for comments on the manuscript. Work in the author's laboratory is supported by the National Institutes of Health (Grant GM 076232).

References

[1] O. Nanba, Ki. Satoh, Proc. Natl. Acad. Sci. U.S.A. 84 (1987) 109.
[2] M.Y. Okamura, Ki. Satoh, R.A. Isaacson, G. Feher, in: J. Biggins (Ed.), Progress in Photosynthesis Research, vol. I, Martinus Nijhoff Publishers, Dordrecht, 1987, p. 379.
[3] K.N. Ferreira, T.M. Iverson, K. Maghlaoui, J. Barber, S. Iwata, Science 303 (2004) 1831.
[4] B. Loll, J. Kern, W. Saenger, A. Zouni, J. Biesiadka, Nature 438 (2005) 1040.
[5] X.-S. Tang, B.A. Diner, Biochemistry 33 (1994) 4594.
[6] T.M. Bricker, J. Morvant, N. Masri, H.M. Sutton, L.K. Frankel, Biochim. Biophys. Acta 1409 (1998) 50.

[8] This particular explanation was first suggested to me by Gary Brudvig.

[7] M.J. Reifler, D.A. Chisholm, J. Wang, B.A. Diner, G.W. Brudvig, in: G. Garab (Ed.), Photosynthesis, Mechanisms and Effects, vol. II, Kluwer Academic Publishers, Dordecht, The Netherlands, 1998, p. 1189.
[8] M. Sugiura, Y. Inoue, Plant Cell Physiol. 40 (1999) 1219.
[9] B.A. Diner, Biochim. Biophys. Acta 1503 (2001) 147.
[10] R.J. Debus, Biochim. Biophys. Acta 1503 (2001) 164.
[11] R.J. Debus, in: T. Wydrzynski, Ki. Satoh (Eds.), Photosystem II: The Light-Driven Water:Plastoquinone Oxidoreductase, Springer, Dordrecht, The Netherlands, 2005, p. 261.
[12] J. Yano, J. Kern, K. Sauer, M.J. Latimer, Y. Pushkar, J. Biesiadka, B. Loll, W. Saenger, J. Messinger, A. Zouni, V.K. Yachandra, Science 314 (2006) 821.
[13] J. Yano, J. Kern, K.-D. Irrgang, M.J. Latimer, U. Bergmann, P. Glatzel, Y. Pushkar, J. Biesiadka, B. Loll, K. Sauer, J. Messinger, A. Zouni, V.K. Yachandra, Proc. Natl. Acad. Sci. U.S.A. 102 (2005) 12047.
[14] M. Grabolle, M. Haumann, C. Müller, P. Liebisch, H. Dau, J. Biol. Chem. 281 (2006) 4580.
[15] C. Zscherp, A. Barth, Biochemistry 40 (2001) 1875.
[16] H. Fabian, W. Mäntele, in: J.M. Chalmers, P.R. Griffiths (Eds.), Handbook of Vibrational Spectroscopy, John Wiley & Sons, Chichester, United Kingdom, 2002, p. 3399.
[17] A. Barth, C. Zscherp, Q. Rev. Biophys. 35 (2002) 369.
[18] A. Barth, Biochim. Biophys. Acta 1767 (2007) 1073.
[19] H.-A. Chu, W. Hillier, N.A. Law, G.T. Babcock, Biochim. Biophys. Acta 1503 (2001) 69.
[20] T. Noguchi, C. Berthomieu, in: T. Wydrzynski, Ki. Satoh (Eds.), Photosystem II: The Light-Driven Water:Plastoquinone Oxidoreductase, Springer, Dordrecht, The Netherlands, 2005, p. 367.
[21] T. Noguchi, Photosyn. Res. 91 (2007) 59.
[22] T. Noguchi, Coord. Chem. Rev. 252 (2008) 336.
[23] P.J. Nixon, J.T. Trost, B.A. Diner, Biochemistry 31 (1992) 10859.
[24] H.-A. Chu, W. Hillier, R.J. Debus, Biochemistry 43 (2004) 3152.
[25] Y. Kimura, N. Mizusawa, T. Yamanari, A. Ishii, T.-A. Ono, J. Biol. Chem. 280 (2005) 2078.
[26] S.Yu. Venyaminov, N.N. Kalnin, Biopolymers 30 (1990) 1243.
[27] R.C. Mehrotra, R. Bohra, Metal Carboxylates, Academic Press, London, UK, 1983.
[28] G.B. Deacon, R.J. Phillips, Coord. Chem. Rev. 33 (1980) 227.
[29] J.E. Tackett, Appl. Spectrosc. 43 (1989) 483.
[30] M. Nara, H. Torii, M. Tasumi, J. Phys. Chem. 100 (1996) 19812.
[31] K. Nakamoto, Infrared and Raman Spectra of Inorganic and Coordination Compounds. Part B. Applications in Coordination, Organometallic, and Bioinorganic Chemistry, John Wiley & Sons, New York, NY, 1997.
[32] M.A. Strickler, L.M. Walker, W. Hillier, R.J. Debus, Biochemistry 44 (2005) 8571.
[33] Y. Kimura, K. Hasegawa, T. Yamanari, T.-A. Ono, Photosynth. Res. 84 (2005) 245.
[34] H. Suzuki, Y. Taguchi, M. Sugiura, A. Boussac, T. Noguchi, Biochemistry 45 (2006) 13454.
[35] E.M. Sproviero, J.A. Gascón, J.P. McEvoy, G.W. Brudvig, V.S. Batista, J. Chem. Theory Comput. 2 (2006) 1119.
[36] J.P. McEvoy, G.W. Brudvig, Chem. Rev. 106 (2006) 4455.
[37] H.-A. Chu, A.P. Nguyen, R.J. Debus, Biochemistry 33 (1994) 6150.
[38] K. Cser, B.A. Diner, P.J. Nixon, I. Vass, Photobiochem. Photobiol. Sci. 4 (2005) 1049.
[39] R.O. Cohen, P.J. Nixon, B.A. Diner, J. Biol. Chem. 282 (2007) 7209.
[40] N. Mizusawa, Y. Kimura, A. Ishii, T. Yamanari, S. Nakazawa, H. Teramoto, T.-A. Ono, J. Biol. Chem. 279 (2004) 29622.
[41] N. Mizusawa, T. Yamanari, Y. Kimura, A. Ishii, S. Nakazawa, T.-A. Ono, Biochemistry 43 (2004) 14644.
[42] M.A. Strickler, W. Hillier, R.J. Debus, Biochemistry 45 (2006) 8801.
[43] H.-A. Chu, R.J. Debus, G.T. Babcock, Biochemistry 40 (2001) 2312.
[44] Y. Kimura, N. Mizusawa, A. Ishii, S. Nakazawa, T.-A. Ono, J. Biol. Chem. 280 (2005) 37895.
[45] H.-A. Chu, H. Sackett, G.T. Babcock, Biochemistry 39 (2000) 14371.
[46] R.J. Debus, M.A. Strickler, L.M. Walker, W. Hillier, Biochemistry 44 (2005) 1367.
[47] P.J. Nixon, B.A. Diner, Biochemistry 31 (1992) 942.
[48] B.A. Diner, P.J. Nixon, Biochim. Biophys. Acta 1101 (1992) 134.
[49] K.A. Campbell, D.A. Force, P.J. Nixon, F. Dole, B.A. Diner, R.D. Britt, J. Am. Chem. Soc. 122 (2000) 3754.
[50] R.J. Debus, C. Aznar, K.A. Campbell, W. Gregor, B.A. Diner, R.D. Britt, Biochemistry 42 (2003) 10600.
[51] H.-A. Chu, A.P. Nguyen, R.J. Debus, Biochemistry 34 (1995) 5839.
[52] H.-A. Chu, A.P. Nguyen, R.J. Debus, Biochemistry 33 (1994) 6137.
[53] J.P. Whitelegge, D. Koo, B.A. Diner, I. Domian, J.M. Erickson, J. Biol. Chem. 270 (1995) 225.
[54] J.S. Vrettos, G.W. Brudvig, Phil. Trans. R. Soc. Lond. B 357 (2002) 1395.
[55] J.P. McEvoy, G.W. Brudvig, Phys. Chem. Chem. Phys. 6 (2004) 4754.
[56] J. Messinger, Phys. Chem. Chem. Phys. 6 (2004) 4764.
[57] M. Lundberg, P.E.M. Siegbahn, Phys. Chem. Chem. Phys. 6 (2004) 4772.
[58] J.P. McEvoy, J.A. Gascón, V.S. Batista, G.W. Brudvig, Photobiochem. Photobiophys. Sci. 4 (2005) 940.
[59] N.D. Chasteen, P.M. Harrison, J. Struct. Biol. 126 (1999) 182.
[60] E.C. Theil, in: A. Messerschmidt, R. Huber, T.L. Poulos, K. Wieghardt (Eds.), Handbook of Metalloproteins, John Wiley & Sons, Chichester, U.K, 2000, p. 771.
[61] S.V. Antonyuk, V.R. Melik-Adamyan, A.N. Popov, V.S. Lamzin, P.D. Hempstead, P.M. Harrison, P.J. Artymyuk, V.V. Barynin, Kristallograpfia 45 (2000) 111 (Engl. Trans., Crystallogr. Rep. 45, 105).
[62] V.V. Barynin, M.M. Whittaker, S.V. Antonyuk, V.S. Lamzin, P.M. Harrison, P.J. Artymiuk, J.W. Whittaker, Structure 9 (2001) 725.
[63] W.C. Liang, T.A. Roelofs, R.M. Cinco, A. Rompel, M.J. Latimer, W.O. Yu, K. Sauer, M.P. Klein, V.K. Yachandra, J. Am. Chem. Soc. 122 (2000) 3399.
[64] M. Haumann, C. Müller, P. Liebisch, L. Iuzzolino, J. Dittmer, M. Grabolle, T. Neisius, W. Meyer-Klaucke, H. Dau, Biochemistry 44 (2005) 1894.
[65] J.H. Robblee, J. Messinger, R.M. Cinco, K.L. McFarlane, C. Fernandez, S.A. Pizarro, K. Sauer, V.K. Yachandra, J. Am. Chem. Soc. 124 (2002) 7459.
[66] M.A. Strickler, L.M. Walker, W. Hillier, R.D. Britt, R.J. Debus, Biochemistry 46 (2007) 3151.
[67] R.J. Debus, K.A. Campbell, D.P. Pham, A.-M.A. Hays, R.D. Britt, Biochemistry 39 (2000) 6275.
[68] K. Clausen, S. Winkler, A.M. Hays, M. Hundelt, R.J. Debus, W. Junge, Biochim. Biophys. Acta 1506 (2001) 224.
[69] V.A. Szalai, G.W. Brudvig, Biochemistry 35 (1996) 15080.
[70] C. Tommos, G.T. Babcock, Biochim. Biophys. Acta 1458 (2000) 199.
[71] K.A. Campbell, J.M. Peloquin, B.A. Diner, X.S. Tang, D.A. Chisholm, R.D. Britt, J. Am. Chem. Soc. 119 (1997) 4787.
[72] R. Hienerwadel, A. Boussac, J. Breton, B.A. Diner, C. Berthomieu, Biochemistry 36 (1997) 14712.
[73] M. Haumann, W. Junge, Biochim. Biophys. Acta 1411 (1999) 121.
[74] S. Styring, Y. Feyziyev, F. Mamedov, W. Hillier, G.T. Babcock, Biochemistry 42 (2003) 6185.
[75] X.-S. Tang, B.A. Diner, B.S. Larsen, M.L. Gilchrist Jr., G.A. Lorigan, R.D. Britt, Proc. Natl. Acad. Sci. U.S.A. 91 (1994) 704.
[76] G.L. Yeagle, M.L. Gilchrist, Jr., L.M. Walker, R.J. Debus, R.D. Britt, Phil. Trans. R. Soc. Lond. B, in press.
[77] M.L. Gilchrist, Jr., Pulsed Electron Paramagnetic Resonance Investigation of Photosynthetic Oxygen Evolution, Ph.D. Dissertation, University of California, Davis, CA, 1996.
[78] R.J. Debus, K.A. Campbell, W. Gregor, Z.-L. Li, R.L. Burnap, R.D. Britt, Biochemistry 40 (2001) 3690.
[79] T. Noguchi, Y. Inoue, X.-S. Tang, Biochemistry 38 (1999) 10187.
[80] Y. Kimura, N. Mizusawa, A. Ishii, T.-A. Ono, Biochemistry 44 (2005) 16072.
[81] P.J. Nixon, B.A. Diner, Biochem. Soc. Trans. 22 (1994) 338.
[82] H.-A. Chu, A.P. Nguyen, R.J. Debus, Biochemistry 34 (1995) 5859.
[83] Y. Allahverdiyeva, Z. Deák, A. Szilárd, B.A. Diner, P.J. Nixon, I. Vass, Eur. J. Biochem. 271 (2004) 3523.
[84] R.J. Debus, K.A. Campbell, J.M. Peloquin, D.P. Pham, R.D. Britt, Biochemistry 39 (2000) 470.
[85] Ka. Satoh, S. Katoh, FEBS Lett. 190 (1985) 199.

[86] A. Boussac, P. Sétif, A.W. Rutherford, Biochemistry 31 (1992) 1224.
[87] V.J. DeRose, C.-H. Kim, W.E. Newton, D.R. Dean, B.M. Hoffman, Biochemistry 34 (1995) 2809.
[88] H.-I. Lee, K.S. Thrasher, D.R. Dean, W.E. Newton, B.M. Hoffman, Biochemistry 37 (1998) 13370.
[89] M.L. Quillin, R.M. Arduini, J.S. Olson, G.N. Phillips Jr., J. Mol. Biol. 234 (1993) 140.
[90] R.L. Haining, B.A. McFadden, Photosynth. Res. 41 (1994) 349.
[91] T.M. Bricker, L.K. Frankel, Photosynth. Res. 72 (2002) 131.
[92] C. Rosenberg, J. Christian, T.M. Bricker, C. Putnam-Evans, Biochemistry 38 (1999) 15994.
[93] M.A. Strickler, H.J. Hwang, R.L. Burnap, J. Yano, L.M. Walker, R. J. Service, R.D. Britt, W. Hillier, R.J. Debus, Phil. Trans. R. Soc. Lond. Ser. B, in press.
[94] T. Noguchi, T.-A. Ono, Y. Inoue, Biochim. Biophys. Acta 1228 (1995) 189.
[95] T. Noguchi, M. Sugiura, Biochemistry 42 (2003) 6035.
[96] Y. Kimura, N. Mizusawa, A. Ishii, T. Yamanari, T.-A. Ono, Biochemistry 42 (2003) 13170.
[97] Y. Taguchi, T. Noguchi, Biochim. Biophys. Acta 1767 (2007) 535.
[98] C.A. McPhalen, N.C.J. Strynadka, M.N.G. James, Adv. Protein Chem. 42 (1991) 77.
[99] E. Pidcock, G.R. Moore, J. Biol. Inorg. Chem. 6 (2001) 479.
[100] M. Qian, L. Dao, R.J. Debus, R.L. Burnap, Biochemistry 38 (1999) 6070.
[101] M. Hundelt, A.-M.A. Hays, R.J. Debus, W. Junge, Biochemistry 37 (1998) 14450.
[102] M. Hundelt, A.-M.A. Hays, R.J. Debus, W. Junge, in: G. Garab (Ed.), Photosynthesis: Mechanisms and Effects, vol. II, Kluwer Academic Publishers, Dordrecht, The Netherlands, 1998, p. 1387.
[103] Z.L. Li, R.L. Burnap, Biochemistry 40 (2001) 10350.
[104] H. Ishikita, W. Saenger, B. Loll, J. Biesiadka, E.-W. Knapp, Biochemistry 45 (2006) 2063.
[105] J.W. Murray, J. Barber, J. Struct. Biol. 159 (2007) 228.
[106] P. Glatzel, U. Bergmann, J. Yano, H. Visser, J.H. Robblee, W. Gu, F.M.F. De Groot, G. Christou, V.L. Pecoraro, S.P. Cramer, V.K. Yachandra, J. Am. Chem. Soc. 126 (2004) 9946.
[107] M. Haumann, P. Liebisch, C. Müller, M. Barra, M. Grabolle, H. Dau, Science 310 (2005) 1019.
[108] L. Kulik, B. Epel, W. Lubitz, J. Messinger, J. Am. Chem. Soc. 127 (2005) 2392.
[109] T.A. Roelofs, W. Liang, M.J. Latimer, R.M. Cinco, A. Rompel, J.C. Andrews, K. Sauer, V.K. Yachandra, M.P. Klein, Proc. Natl. Acad. Sci. U.S.A. 93 (1996) 3335.
[110] J. Messinger, J.H. Robblee, U. Bergmann, C. Fernandez, P. Glatzel, H. Visser, R.M. Cinco, K.L. McFarlane, E. Bellacchio, S.A. Pizarro, S.P. Cramer, K. Sauer, M.P. Klein, V.K. Yachandra, J. Am. Chem. Soc. 123 (2001) 7804.
[111] A. Barth, Prog. Biophys. Mol. Biol. 74 (2000) 141.
[112] H. Visser, C.E. Dubé, W.H. Armstrong, K. Sauer, V.K. Yachandra, J. Am. Chem. Soc. 124 (2002) 11008.
[113] A. Cua, J.S. Vrettos, J.C. de Paula, G.W. Brudvig, D.F. Bocian, J. Biol. Inorg. Chem. 8 (2003) 439.
[114] K. Hasegawa, T.-A. Ono, Bull. Chem. Soc. Jpn. 79 (2006) 1025.